sustainability

MDPI

Article

Indicator Construction of Road Surface Deformation Activity in Cold Regions and Its Relationship with the Distribution and Development of Longitudinal Cracks

Hao Wang [1], Lun Ji [2,*], Hongju Zhang [3], Yuqi Lou [4], Linlin Xu [2] and Yiqiu Tan [2]

[1] Heilongjiang Province Highway Engineering Cost Management Bureau, Harbin 150016, China; chinafreeway@126.com
[2] School of Traffic Science and Engineering, Harbin Institute of Technology, Harbin 150090, China; xulinlincam@126.com (L.X.); yiqiutan@hit.edu.cn (Y.T.)
[3] Heilongjiang Provincial Longjian Road & Bridge the 1st Engineering Co., Ltd., Harbin 150028, China; jilunhit@126.com
[4] Heilongjiang Bada Road and Bridge Construction Co., Ltd., Harbin 150001, China; guoyoufei@126.com
* Correspondence: jilun@hit.edu.cn

Abstract: As a type of road distress in cold areas, longitudinal cracks have a high incidence and cause serious damage. The occurrence of longitudinal cracks is related to the conditions of the subgrade, pavement structure, material properties, and water temperature. The goal is to gain a deeper understanding of the occurrence mechanism of longitudinal cracks and provide references for the prevention and control of longitudinal cracks. Through the monitoring of vertical deformation, longitudinal crack distribution, and the development of typical roads in cold areas, the discrete characteristics and the variance in the distribution of deformations were analyzed. The construction of an activity index based on the variance of time-series elevation and the standard deviation of elevation change was used to describe the activity level of road sections, longitudinal lines, intervals, and longitudinal deformation. Based on the correlation between vertical deformation and longitudinal cracks on the road surface, the relationships among the activity, condition, distribution, and development characteristics of longitudinal cracks were analyzed. The results indicate that there were significant differences in the deformation activity of the road surface at different times and that the activity was greater during the freezing and thawing periods. The development and distribution characteristics of longitudinal cracks were significantly correlated with activity level. This study can help improve our understanding of the dynamic deformation characteristics of road surfaces under natural conditions and the relationship between transverse distribution differences and longitudinal cracks. It can also provide clarifications and references for the development of the roadbed, pavement structure and materials, the mechanics of the pavement structure, the emergence of distresses, and the laws of development in cold areas.

Keywords: cold regions; longitudinal crack; vertical deformation; activity; distribution characteristics

Citation: Wang, H.; Ji, L.; Zhang, H.; Lou, Y.; Xu, L.; Tan, Y. Indicator Construction of Road Surface Deformation Activity in Cold Regions and Its Relationship with the Distribution and Development of Longitudinal Cracks. *Sustainability* **2023**, *15*, 15466. https://doi.org/10.3390/su152115466

Academic Editor: Marinella Giunta

Received: 19 June 2023
Revised: 21 September 2023
Accepted: 27 September 2023
Published: 31 October 2023

1. Introduction

The temperature, water levels, and external environment constantly change in seasonal frozen soil regions, and this complex process produces the frost thaw of the soil and changes in its properties [1], resulting in the migration of water [2], the frost heave and thaw collapse of the road base, and the thawing and sinking effect [3], resulting in the frost thaw deformation of the foundation of the transport infrastructure [4,5]. This deformation occurs as an inhomogeneous deformation in the longitudinal and transversal directions of the road [6], causing longitudinal cracks and other issues, which are the main cause of transport infrastructure problems [7].

Compared with other regions, the deformation in cold regions is dynamic with high frequency and amplitude [8]. As a typical road condition, longitudinal cracks are induced by external factors such as uneven deformation and stress under the action of various factors, as well as the characteristics of the asphalt pavement itself, such as the void ratio, the content of effective binder, and the PG grade [9]. Thus, frost heave and thaw collapse of the roadbed pavement is the direct causative factor, whereas the condition is related to the intensity of the frost heave and thaw collapse and the ability of the pavement to resist deformation and cracking. In addition, structural or material heterogeneity caused by reconstruction and expansion [10], and vertical deformation of the roadbed influenced by the orientation of road structures [11,12] can trigger longitudinal cracks. These factors act cyclically and repeatedly [13–15].

The deformation triggered by freezing and thawing acts on the road structure and its active characteristics and distribution characteristics are of positive significance for the study of reasonable pavement structure and materials, the analysis of the whole process of structural performance, and the whole life cycle evaluation [16]. It is very important to accurately analyze the structural mechanical response of the pavement, to reasonably design the pavement structure and materials, to reduce the occurrence of diseases, and to prolong the life of the road in service. Batenipour H studied the performance of 18 km of road embankment in an area of discontinuous permafrost. Measurements of ground temperatures indicate that previously ice-rich foundation soils have melted the side slopes at the toe. The results provide insight into the causes of embankment deformation [17]. Linares C.M. conducted research on various properties of asphalt concrete pavements and also discussed the effect of freeze–thaw cycles on the stability of asphalt mixtures [18]. Simonsen E. provided a review of the literature related to soil thawing and pavement-bearing capacity during spring thaw. The literature reviewed suggested that there are numerous parameters (soil type, permeability, drainage conditions, and thaw rate) that influence the degree of weakening during spring thawing. However, the relative importance of these factors was not known, and the literature on large-scale field trials suggests considerable variation in pavement performance during thaw weakening [19]. Liu J. analyzed the thermal state and thawing and sinking characteristics of the roadbed based on monitoring data from three sections of the new republic and found that the rate of permafrost thawing is linearly and positively correlated with the mean annual ground temperature [20]. Previously, researchers have analyzed the freeze–thaw characteristics and longitudinal crack condition through indoor experiments and on-site research and monitoring [21], while the research in this area had a shorter period. The monitoring also did not pay attention to the differences in deformation on the transverse cross-section and active characteristics and did not pay attention to the distribution characteristics of the longitudinal cracks in the transverse direction or the characteristics of the development of the longitudinal cracks. Therefore, this aspect of the analysis needs to be strengthened. In addition, with the increase in road reconstruction expansion projects and lane and pavement width, the deformation and mechanical characteristics of the research needs will be more prominent [22].

This paper selected non-expansion highway segments. The method of selecting monitoring sections and using monitoring data to analyze the distribution and development of longitudinal cracks is also applicable in foreign countries. The characteristics of road surface vertical deformation were analyzed; indicators of the activity of road surface vertical deformation were established through the monitoring of the distribution and development of vertical deformation and longitudinal cracks on typical roads in cold regions; and the relationship between the activity and the condition, distribution, and development characteristics of longitudinal cracks was analyzed. This article provides a benchmark for the study of materials, structures, and distresses related to road engineering. Pavement life can be extended by reducing longitudinal cracks. The cost of road maintenance can be reduced by timely detection and repair of longitudinal cracks. This contributes to the sustainable development of roads.

2. Field Monitoring Results

2.1. Test Section

The most effective means of conducting a roadway surface deformation study is to monitor the roadway surface in the field [23,24]. Three typical road sections were selected through field research, and the selected sections were all semi-rigid base asphalt pavements.

In order to record the vertical relative deformation changes of the pavement in the transverse and longitudinal directions more completely, three cross sections were set up in the longitudinal direction of each monitoring section at 30 m intervals, and six monitoring points were set up in each cross section. A total of five monitoring points were set up at the edge of the lane and the middle of the lane in the overtaking lane and the carriageway. One monitoring point was set up at the distance of half of the carriageway, extending from the edge of the carriageway to the emergency lane. On the shoulder side of the road towards the central divider, the monitoring points were numbered from 1 to 6 in order, as shown in Figure 1.

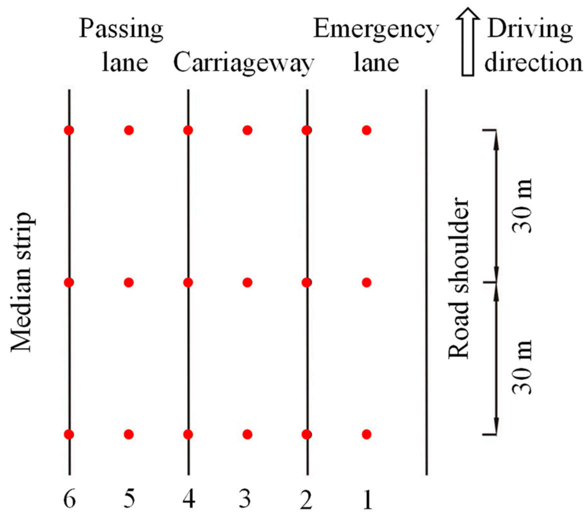

Figure 1. Layout of road vertical relative deformation monitoring points.

By means of the field survey, the distress occurring on the road was documented, as shown in Table 1.

The solid structure with negligible frost heave displacement was selected as the reference level by the electronic digital level used in the elevation monitoring equipment. Regular elevation monitoring and distress surveys were carried out.

2.2. Road Surface Deformation Characteristics

Using the datum level elevation data as the initial value, the elevation data measured in different periods was subtracted from it. The difference was the vertical relative deformation of the pavement, and the formula for calculating it is shown as Equations (1) and (2):

$$\Delta H_{i,\,j} = H_{i,\,j} - H_{i,\,0} \tag{1}$$

$$\bar{H}_j = \frac{1}{n}\sum_{i=1}^{n} \Delta H_{i,\,j} \tag{2}$$

where:

ΔH_i—The relative vertical relative deformation value produced at a point (j) at the ith point on the cross-section, $i = 1, 2 \cdots, 6$.

$\bar{H}_j$—The average vertical relative deformation value at a moment (j) in the cross section.

H_{ij}—The elevation of the ith point on the transect at a given moment (j).

H_{i0}—The elevation of the reference level at the ith point on the transect.

The calculation results are shown in Figure 2.

Table 1. Survey results of the road distress.

Serial Number	Monitoring Locations	Distress Information
#3	G1001 East Ring Road K68 + 150–K68 + 210 (Jiangbei direction) The monitoring sections were: G, H, and I.	There are six linear longitudinal cracks with a regular alignment, with one of them incurring map cracks accompanied by rutting. Four cracks were located in the middle lane, with staggered development at the transverse cracks. One longitudinal crack of 60 m in the inner overtaking lane ran through the investigated section. Another longitudinal crack of 46 m was distributed in the outer emergency lane. There were nine transverse cracks, predominantly long cracks, with five transverse cracks exceeding 7.5 m.
#4	G1001 East Ring K88 + 166.4–K88 + 226.4 (Wapengyao direction)The monitoring sections were: J, K, and L.	There were 6 linear longitudinal cracks, 2 of 60 m, 2 in the range of 30–40 m in length, and the other 2 within 10 m in length. There were 14 transverse cracks, with 11 running through the outer emergency lane and cutting off at the location of the longitudinal cracks. The distribution of the transverse cracks was more evenly spaced and concentrated in the outer emergency lane.
#9	G202 Ha Wu Road K652 + 100–K652 + 160 (Harbin direction) The monitoring sections were: Y, Z, and AAI	The longitudinal cracks struck regularly in a straight line, with only one crack of 60 m in length, one of 12 m in length, and the others being short cracks of no more than 6 m in length. Longitudinal cracks were mainly distributed in the middle lane. There were five transverse cracks, with three cracks running through the roadway and two cracks within 4–8 m in length. There was one small area of pockmark.

Note: Combined with Figure 1 and Table 1, taking the #3 highway as an example, the monitoring points of the monitoring section G were numbered as G1, G2, G3, G4, G5, and G6.

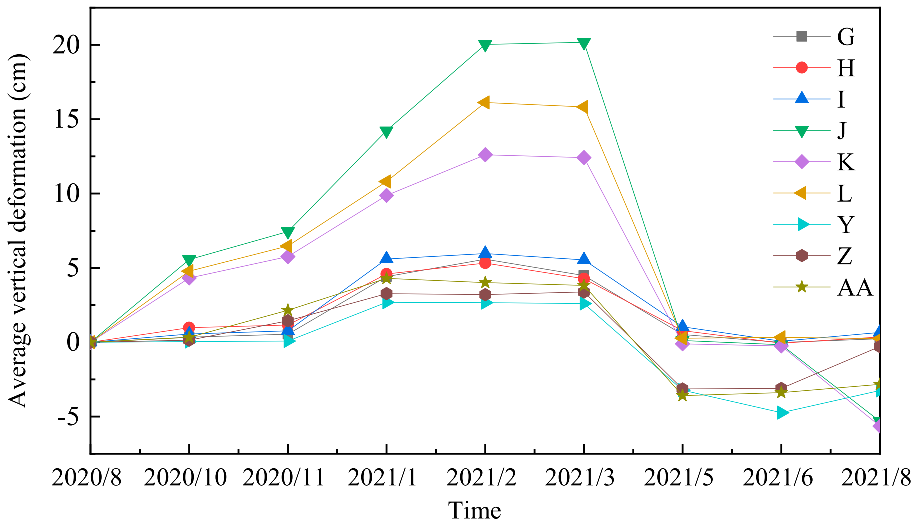

Figure 2. The average vertical deformation of cross-sectional changes with time.

2.3. Monitoring Results of Longitudinal Crack Conditions

2.3.1. Length and Growth Trends of Longitudinal Cracks

Crack monitoring was conducted in conjunction with elevation monitoring. During the tests, all cracks were initially investigated and the lengths were recorded. Thereafter, the lengths of new cracks were recorded in comparison. Crack monitoring of some sections is shown in Figure 3.

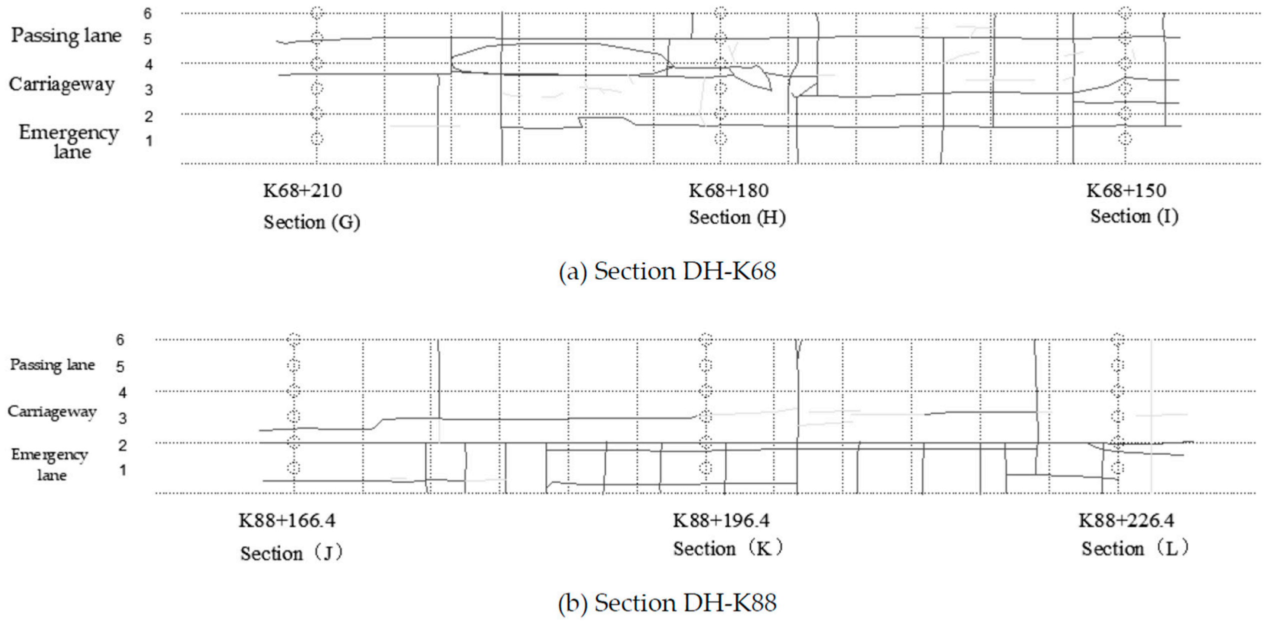

Figure 3. Initial conditions of cracks in typical sections.

The monitoring results for each typical section are shown in Table 2.

Table 2. Monitoring results of longitudinal cracks length.

Date of Monitoring	Monitoring Time (d)	Length of Longitudinal Cracks (m)		
		DH Expressway K68	DH Expressway K88	HW Highway K652
20 August 2020	0.0	176.2	235.0	100.4
7 November 2020	77.0	180.3	238.6	103.2
23 February 2021	183.0	182.2	241.3	105.4
22 May 2021	273.0	183.6	244.0	106.3
16 August 2021	357.0	184.0	248.0	110.0

As can be seen from Table 3, the cracks continued to grow overall, with different growth rates rising at each stage, using the length of growth per 10 days as the rate of longitudinal crack development. Table 4 below shows the rate of longitudinal crack development.

Table 3. Development rate of longitudinal cracks.

Time Period	Longitudinal Crack Development Rate (m/10 d)		
	DH Expressway K68	DH Expressway K88	HW Highway K652
Aug.–Nov.	0.53	0.47	0.36
Nov.–Feb.	0.18	0.25	0.21
Feb.–May	0.16	0.30	0.10
May.–Aug.	0.05	0.48	0.44

Table 4. Difference in time-series elevation change (m).

Difference in Time-Series Elevation Change	Jan. 2021–Aug. 2020	Feb. 2021–Jan. 2021	Mar. 2021–Feb. 2021	May 2021–Mar. 2021	Jun. 2021–May 2021	Aug. 2021–Jun. 2021
G1	0.0404	0.0134	−0.0084	−0.0393	−0.0036	0.0003
G2	0.0405	0.0154	−0.0091	−0.0404	−0.0037	0.0008
G3	0.0427	0.0113	−0.0137	−0.0346	−0.0034	0.0002
G4	0.0462	0.0100	−0.0159	−0.0343	−0.0063	0.0030
G5	0.0490	0.0089	−0.0146	−0.0397	−0.0075	0.0042
G6	0.0456	0.0115	−0.0042	−0.0492	−0.0082	0.0068
H1	0.0523	0.0026	−0.0062	−0.0412	−0.0064	0.003
H2	0.0510	0.0053	−0.0119	−0.0348	−0.0081	0.0027
H3	0.0459	0.0072	−0.0161	−0.0294	−0.0085	0.0026
H4	0.0458	0.0076	−0.0129	−0.0324	−0.0089	0.0041
H5	0.0427	0.0113	−0.0101	−0.0371	−0.0080	0.0047
H6	0.0379	0.0103	−0.006	−0.0353	−0.0106	0.0080
I1	0.0612	0.0014	−0.0081	−0.0427	−0.0094	0.0047
I2	0.0637	0.0005	0.0089	−0.0595	−0.0110	0.0054
I3	0.0556	0.0013	0.0090	−0.0560	−0.0084	0.0044
I4	0.0562	0.0010	−0.0157	−0.0303	−0.0118	0.0066
I5	0.0541	0.0067	−0.0120	−0.0401	−0.0085	0.0064
I6	0.0455	0.0104	−0.0072	−0.0413	−0.0094	0.0084
J1	0.1197	0.0556	0.0024	−0.1776	−0.0008	−0.0528
J2	0.1408	0.0604	0.002	−0.2037	−0.0026	−0.0524
J3	0.1514	0.0628	0.0002	−0.2173	−0.0027	−0.0498
J4	0.1498	0.0595	−0.0004	−0.2100	−0.0030	−0.0508
J5	0.1511	0.0575	0.0020	−0.2042	−0.0043	−0.0508
J6	0.1412	0.0520	0.0021	−0.1898	−0.0046	−0.0513
K1	0.0991	0.0364	−0.0010	−0.1379	−0.0003	−0.0541
K2	0.1006	0.0352	−0.0010	−0.1384	−0.0026	−0.0519
K3	0.1033	0.0343	−0.0017	−0.1392	−0.0004	−0.0539
K4	0.0920	0.0333	−0.0012	−0.1303	−0.0007	−0.0533
K5	0.0869	0.0313	−0.0028	−0.1083	−0.0043	−0.0545
K6	0.1107	−0.0065	−0.0039	−0.0966	−0.0011	−0.0557
L1	0.1019	0.0561	−0.0037	−0.1491	0.0003	−0.0011
L2	0.1103	0.0624	−0.0031	−0.1688	0.0025	−0.0026
L3	0.1070	0.0596	0.0006	−0.1677	0.0012	−0.0006
L4	0.1070	0.0536	−0.0012	−0.1609	0.0002	0.0006
L5	0.1120	0.0458	−0.0043	−0.1481	−0.0014	0.0009
L6	0.1100	0.0413	−0.0054	−0.1393	0.0006	−0.0018
Y1	0.0239	−0.0017	−0.0069	−0.0493	−0.0226	0.0232
Y2	0.0283	0.0016	0.0011	−0.0620	−0.0214	0.0196
Y3	0.0358	−0.0009	−0.0003	−0.0677	−0.0209	0.0201
Y4	0.0333	−0.0014	0.0002	−0.0653	−0.0208	0.0201
Y5	0.0250	−0.0012	0.0008	−0.0544	−0.0038	0.0025
Y6	0.0148	0.003	0.0009	−0.0512	−0.0011	0.0039
Z1	0.0223	0.0062	0.0020	−0.0607	0.0005	−0.0012
Z2	0.0308	0.0039	0.0030	−0.0706	0.0022	0.0020
Z3	0.0404	−0.0006	0.0022	−0.0734	0.0006	0.0009
Z4	0.0413	−0.0030	0.0009	−0.0710	0.0011	0.0018
Z5	0.0354	−0.0063	0.0023	−0.0624	−0.0027	0.0059
Z6	0.0261	−0.0044	0.0004	−0.0532	0.0004	0.0032
AA1	0.0380	−0.0034	−0.0017	−0.0667	0.0003	0.0051
AA2	0.0433	−0.0014	−0.0032	−0.0741	0.0040	0.0036
AA3	0.0462	−0.0056	−0.0022	−0.0777	0.0006	0.0065
AA4	0.0519	−0.0030	−0.0032	−0.0859	0.0067	0.0049
AA5	0.0437	−0.0028	−0.0008	−0.0745	0.0017	0.0051
AA6	0.0350	−0.0014	−0.0002	−0.0659	−0.0008	0.0075

2.3.2. Distribution Laws of Longitudinal Cracks

In terms of crack locations, longitudinal cracks appeared on all three lanes, with some cracks more evenly distributed across the three lanes in some sections (e.g., G1011 Hatong high speed K64 + 570–K64 + 630 (Chang'an direction)), some cracks concentrated on the outer emergency lane in some sections (e.g., East Ring G1001 K88 + 166.4–K88 + 226.4 (Wabangyao direction)), and some concentrated on the middle lane road median in some sections (e.g., Hartung high-speed G1011 K59 + 701.5–K59 + 761.5 (Chang'an direction)). To facilitate the analysis of the distribution of longitudinal cracks in the transverse direction, the lengths of the cracks were counted separately for all the longitudinal cracks between point 1 and point 6 on the road section, according to the interval, as shown in Figure 4.

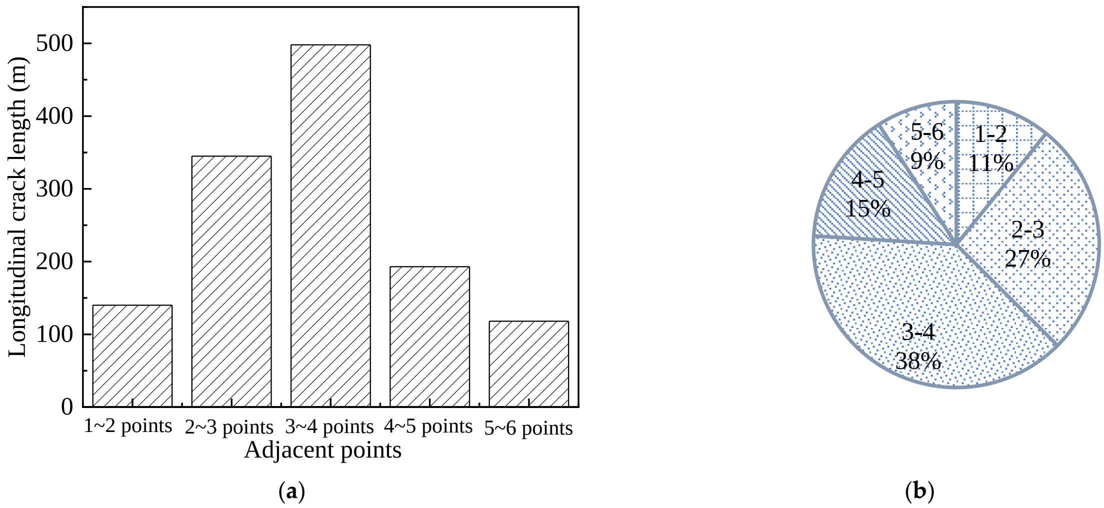

Figure 4. (**a**) Transverse distribution and (**b**) proportional condition of longitudinal cracks.

According to Figure 4, the longitudinal cracks were most severe between points 3 and 4, followed by points 2–3. The length of the longitudinal cracks on the middle carriageway far exceeds the length of the inner overtaking lane and the outer emergency lane. The lengths of the longitudinal cracks between point 1 and point 3 exceed those between point 4 and point 6, indicating that the longitudinal cracking on the shoulder side of the road was more severe than on the median side.

3. Calculation of Deformation Changes and Variances of Monitoring Data

3.1. Calculation of the Difference in Time-Series Elevation Change

Based on monitoring data, the activity analysis methodology was proposed. This method allowed for the analysis of the variance of the deformation data and the degree of deformation activity in the relevant area.

The difference in elevation change between the different monitoring moments and the previous monitoring moment is listed in Table 4, based on Equation (3).

$$\Delta h_{i,\,j} = \Delta H_{i,\,j+1} - \Delta H_{i,\,j} \tag{3}$$

3.2. Standard Deviation of Elevation Differences

(1) Standard deviation calculation of the difference in elevation change between periods for each monitoring section.

The standard deviation of the elevation difference for different periods at each monitoring section was calculated according to Equation (4).

$$\sigma = \sqrt{\frac{1}{N}\sum_{i=1}^{N}(x_i - u)^2} \tag{4}$$

The descriptions of the parameters in the formulae are omitted. The results are shown in Table 5.

Table 5. Standard deviation of the differences in elevation change at different periods at the monitoring sections (unit: m).

Cross-Section	Jan. 2021–Aug. 2020	Feb. 2021–Jan. 2021	Mar. 2021–Feb. 2021	May 2021–Mar. 2021	Jun. 2021–May 2021	Aug. 2021–Jun. 2021
G	0.0031	0.0021	0.0041	0.0049	0.0020	0.0024
H	0.0049	0.0029	0.0036	0.0037	0.0012	0.0019
I	0.0058	0.0037	0.0097	0.0099	0.0013	0.0013
J	0.0110	0.0035	0.0011	0.0131	0.0012	0.0010
K	0.0077	0.0152	0.0011	0.0166	0.0014	0.0012
L	0.0033	0.0074	0.0020	0.0109	0.0012	0.0012
Y	0.0093	0.0031	0.0024	0.0095	0.0095	0.0074
Z	0.0070	0.0045	0.0009	0.0071	0.0015	0.0022
AA	0.0055	0.0014	0.0011	0.0068	0.0025	0.0012

(2) Standard deviation calculation of the elevation differences between different periods at monitoring points as shown in Table 6.

Table 6. Calculation of standard deviation of point elevation change differences (unit: m).

Points	Standard Deviation	Points	Standard Deviation	Points	Standard Deviation
G1	0.0239	J1	0.0924	Y1	0.0255
G2	0.0245	J2	0.1058	Y2	0.0298
G3	0.0236	J3	0.1126	Y3	0.0330
G4	0.0249	J4	0.1097	Y4	0.0317
G5	0.0269	J5	0.1080	Y5	0.0240
G6	0.0282	J6	0.1007	Y6	0.0213
H1	0.0275	K1	0.0736	Z1	0.0260
H2	0.0260	K2	0.0738	Z2	0.0312
H3	0.0237	K3	0.0748	Z3	0.0339
H4	0.0240	K4	0.0693	Z4	0.0332
H5	0.0242	K5	0.0617	Z5	0.0292
H6	0.0224	K6	0.0636	Z6	0.0239
I1	0.0309	L1	0.0772	AA1	0.0311
I2	0.0361	L2	0.0862	AA2	0.0348
I3	0.0326	L3	0.0848	AA3	0.0367
I4	0.0274	L4	0.0819	AA4	0.0409
I5	0.0284	L5	0.0781	AA5	0.0350
I6	0.0261	L6	0.0744	AA6	0.0303

4. Activity Definition and Calculation Results

4.1. Definition of Activity

The standard deviation is the square root of the variance and is represented by the symbol σ, as shown in Equation (4). The standard deviation indicates the degree of dispersion of a set of values. The larger the standard deviation, the larger the deviation of the group's values from the mean, and the smaller the standard deviation, the closer the values are to the mean.

The standard deviation can be used to characterize the degree of dispersion of elevation change, defined as "activity", abbreviated as "act" to describe the degree of activity of elevation change over time by considering time and location for points, lines, and sections. This corresponds to the "activity of a point, line, or section". For example, the activity of point 1 (i = 1) in section G is the standard deviation of the difference in elevation at that point at all times, as shown in Table 7. Equation (5) for the single point activity is as follows:

$$\mathrm{Atv}_{\mathrm{G,i}} = \sigma_{\mathrm{G,i}} \tag{5}$$

Table 7. Results of longitudinal line activity and section longitudinal activity (unit: m).

Longitudinal Number	East Ring K 68 Filling	East Ring K 88 Excavation	Ha-wu Filling
1	0.0273	0.0810	0.0277
2	0.0290	0.0887	0.0320
3	0.0267	0.0907	0.0343
4	0.0253	0.0870	0.0353
5	0.0263	0.0827	0.0293
6	0.0257	0.0797	0.0250
Section longitudinal activity	0.0269	0.0860	0.0317

The activity of each point is averaged according to the longitudinal line number, and the value characteristics of the activity of the elevation changes of the longitudinal line correspond to the longitudinal number. The value is defined as the longitudinal line activity. For example, the activity of the number 1 longitudinal line in section K 68 of the Eastern Ring as shown in Equation (6).

$$\mathrm{Atv}_{ZDHk68,1} = \mathrm{Atv}_{G,1} + \mathrm{Atv}_{H,1} + \mathrm{Atv}_{I,1} \tag{6}$$

The mean value of the activity of each longitudinal line is characteristic of the longitudinal activity of the difference in elevation of the section and is called the longitudinal activity of the section. For instance, the longitudinal activity of section K 68 in the Eastern Ring is shown in Equation (7).

$$\mathrm{Atv}_{ZDHk68} = \sum_{i=1}^{6} \mathrm{Atv}_{ZDHk68,i} \tag{7}$$

4.2. Longitudinal Line Activity and Section Vertical Activity

According to Equation (7), the activity of each longitudinal line and the vertical activity values for the three sections were calculated and the results are shown in Table 7.

Figure 5 shows that there were differences in activity across the longitudinal lines and significant differences in longitudinal line activity across the sections, and the differences could be 3 to 4 times. Taking longitudinal line 3 as an example, the activity of East Ring K68 was 0.0267, Ha Wulu was 0.0343, and East Ring K88 was 0.0907, which was 3.4 times and 2.6 times that of the previous two.

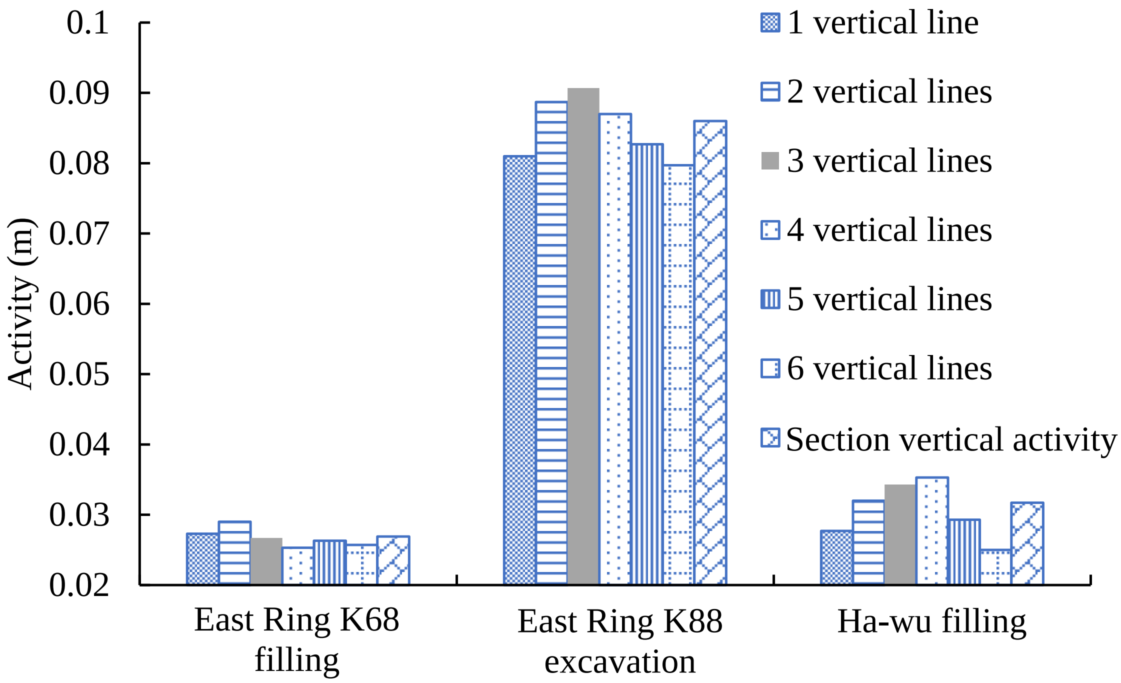

Figure 5. Longitudinal line activity and section longitudinal activity.

5. Relationship between Activity and Longitudinal Cracks

5.1. Longitudinal Line Activity

The longitudinal line activity of each section was averaged according to the line number to obtain the longitudinal activity of the 6 lines for 3 sections, called the total longitudinal activity.

The analysis was carried out according to the four levels of most active (2 longitudinal lines), moderately active (1 longitudinal line), slightly active (2 longitudinal lines), and least active (1 longitudinal line), in order of the largest to smallest standard deviation. The results in Table 8 are organized in accordance with the four activity criteria.

Table 8. Summary of total activity analysis.

Longitudinal Number	Total Activity/m	Three Section Analysis	East Ring K68 Filling	East Ring K88 Excavation	Ha-wu Filling
1	0.045	Slightly active	Most active	Slightly active	Slightly active
2	0.050	Most active	Most active	Most active	Moderately active
3	0.051	Most active	Moderately active	Most active	Most active
4	0.049	Moderately active	Least active	Moderately active	Most active
5	0.046	Slightly active	Slightly active	Slightly active	Slightly active
6	0.043	Least active	Slightly active	Least active	Least active

For the three sections, the longitudinal number 2 and 3 longitudinal lines were the most active. This was followed by longitudinal line number 4, as shown in Figure 6.

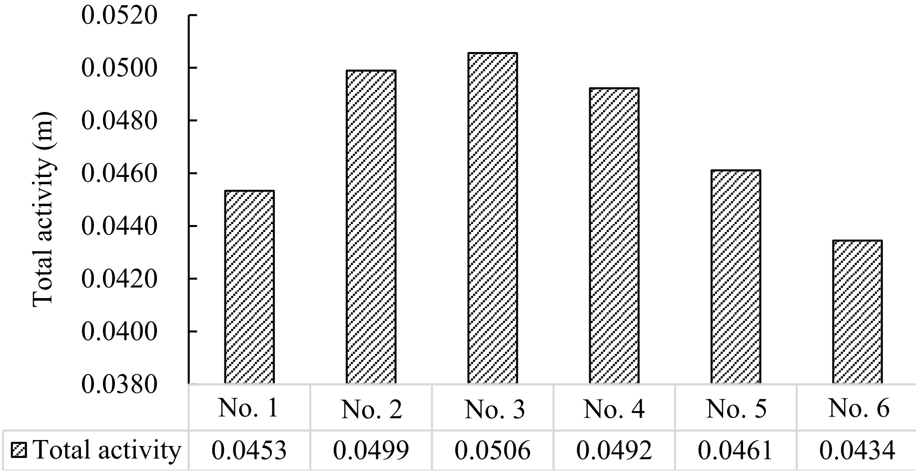

Figure 6. Total activity situation.

As can be seen from Figure 6, lines 2, 3, and 4 were the most active, especially lines 2 and 3. The adjacent lines were less active, which was consistent with the continuity of the road surface. This was also in line with the continuity of the road table. Its distribution characteristics were consistent with Figure 4. The relationship between activity and longitudinal fissures will be analyzed below.

5.2. Relationship between Activity and Longitudinal Crack Lengths

Combining the data in Tables 3 and 8, the annual growth length of longitudinal cracks was in relation to the activity of the sections, as shown in Figure 7.

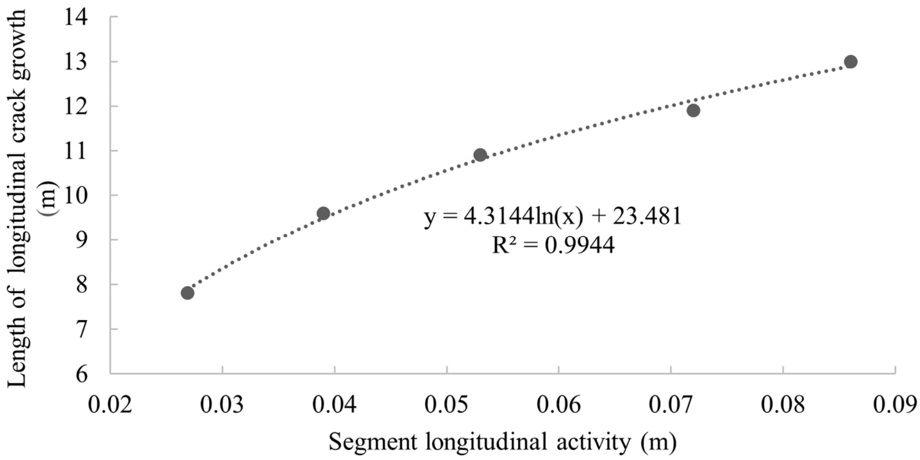

Figure 7. Relationship between annual growth length of longitudinal cracks and section longitudinal activity.

Figure 7 indicates that there is a logarithmic relationship between the annual growth length of longitudinal cracks and section longitudinal activity. The greater the activity, the greater the annual growth length of longitudinal cracks.

5.3. Relationship between Activity and Longitudinal Crack Distribution Characteristics

As can be seen from Table 8 and Figure 4, the classification of the activity classes of the longitudinal lines was consistent across the sections, i.e., the longitudinal lines were active in generally consistent locations. The relationship between the activity level and the distribution characteristics of the longitudinal cracks is analyzed below.

Note that the longitudinal lines connected by monitoring points were used for analysis. Crack monitoring counts the length of cracks in the intervals between points and requires interval activity to be assigned. As the pavement is a continuous structure in the transverse direction, the interval activity was considered the average of the activity of the adjacent longitudinal lines. The results of the summary analysis are shown in Table 9.

Table 9. Total activity and length of longitudinal crack distribution.

Longitudinal Number	1 Longitudinal Line	2 Longitudinal Lines	3 Longitudinal Lines	4 Longitudinal Lines	5 Longitudinal Lines	6 Longitudinal Lines
Total activity(m)	0.0453	0.0499	0.0506	0.0492	0.0461	0.0434
Point Intervals	1–2	2–3	3–4	4–5	5–6	
Interval activity(m)	0.0476	0.0502	0.0499	0.0477	0.0448	
Length of longitudinal cracks(m)	140	345	498	193	118	

In Figure 8, there is a correlation between the crack length and the total activity in the interval. The greater the total activity, the greater the longitudinal crack length. The total activity and length of longitudinal crack follow an exponential relationship.

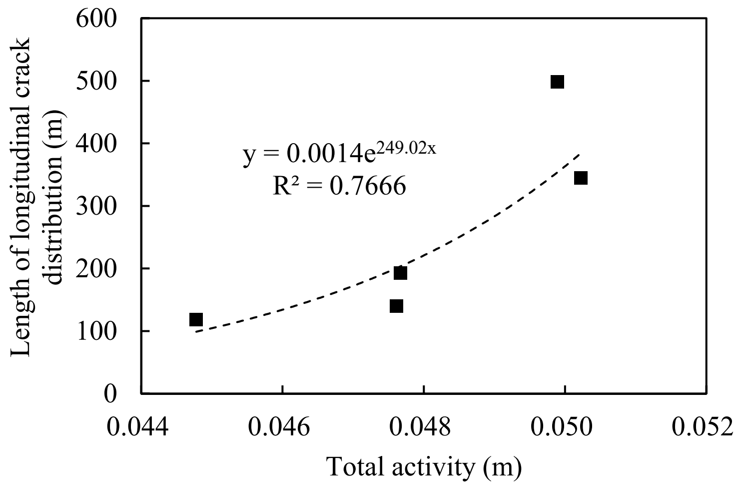

Figure 8. Relationship between total activity and length of longitudinal crack distribution.

5.4. Relationship between Activity and Longitudinal Crack Development in Different Periods of the Section

The results of the different periods of activity of the sections are calculated according to Table 7, as shown in Table 10 below.

Table 10. Activity at different periods of the monitored sections (unit: m).

Section	Jan. 2021–Aug. 2020	Feb. 2021–Jan. 2021	Mar. 2021–Feb. 2021	May 2021–Mar. 2021	Jun. 2021–May 2021	Aug. 2021–Jun. 2021
DH expressway K68	0.0046	0.0029	0.0058	0.0062	0.0015	0.0019
DH expressway K88	0.0073	0.0087	0.0014	0.0136	0.0013	0.0011
HW expressway K652	0.0073	0.0030	0.0015	0.0078	0.0045	0.0036

In Figure 9, each monitoring section is most active from Mar. to May, corresponding to the road thaw and collapse period. And from Aug. to Jan., during the period of thermal expansion and frost heave, activity is relatively greater.

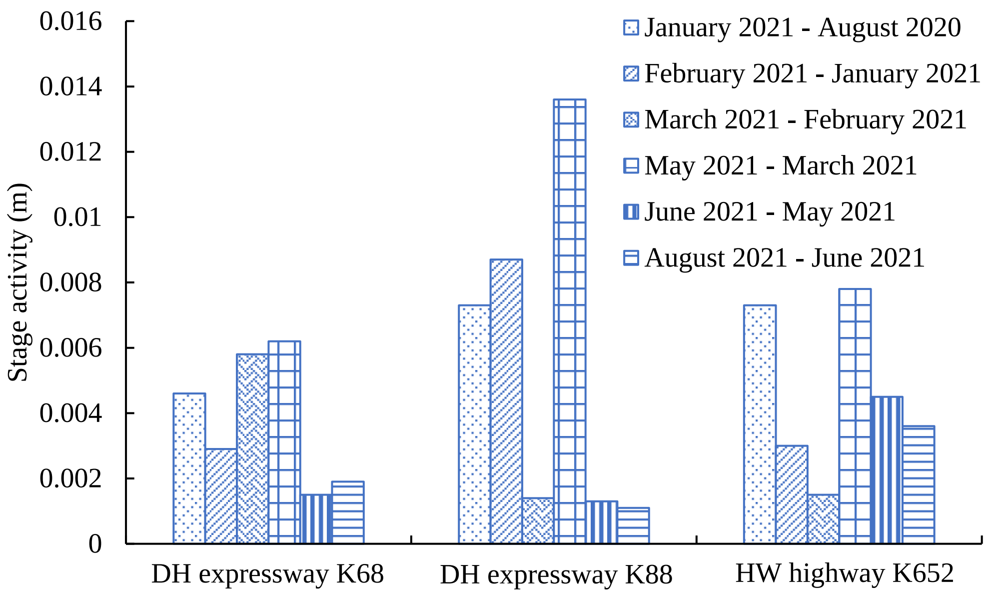

Figure 9. Section activity at different periods.

The relationship between the different time periods of activity and the development of longitudinal cracks was analyzed in conjunction with Tables 8–10. As the longitudinal crack survey was not synchronized with the road surface deformation, the deformation activity of different periods was estimated by using the average of the relevant periods of activity. The results are shown in Table 11 below.

Table 11. Activity and development of longitudinal fissures at different periods.

Time Period	Longitudinal Crack Development Rate (m/10d)			Activity (m)		
	DH Expressway K68	DH Expressway K88	HW Highway K652	DH Expressway K68	DH Expressway K88	HW Highway K652
Aug.–Nov.–Feb.	0.3300	0.3400	0.2700	0.0038	0.0080	0.0052
Feb.–May	0.1600	0.300	0.1000	0.0060	0.0075	0.0047
May to Aug.	0.0500	0.4800	0.4400	0.0017	0.0012	0.00405

This is plotted as follows in Figure 10:

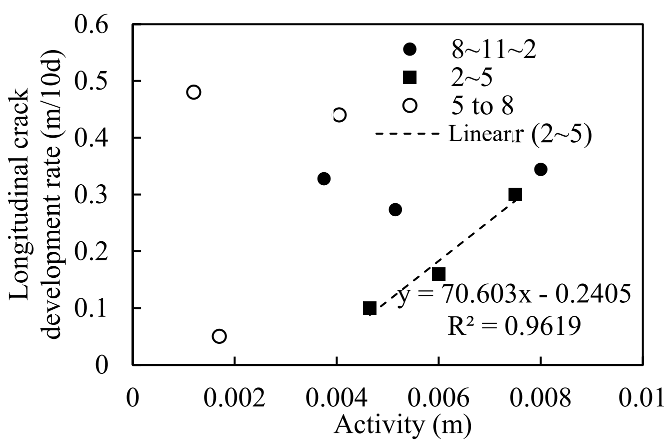

Figure 10. Relationship between activity and longitudinal crack development at different periods.

There is no significant relationship between activity and longitudinal crack development except for February to May, showing a linear relationship. In contrast, the annual growth length of longitudinal cracks in the analysis of Section 4.2 of the article is significantly related to the section longitudinal activity. The analysis suggests that the road experienced frost heave and thaw collapse from February to May. During this period, the activity was higher, and the cracks were fully developed and more pronounced compared to the other periods. This is also reflected in another way: there is a lag between deformation and the appearance of cracks, i.e., the development of cracks needs to go through a certain development process.

6. Conclusions

The methods of selecting monitoring sections and using monitoring data to analyze the distribution and development of longitudinal cracks are also applicable in foreign countries. Through long-term monitoring and data analysis of vertical deformation and longitudinal cracks on several roads in cold regions, a deformation activity index was established to describe the active degree of pavement deformation and distribution characteristics. Therefore, in the engineering design and subject research of subgrade and pavement structure and materials, it is necessary to fully consider the deformation characteristics and active conditions of road surfaces in different regions and their influence on the subgrade and pavement. Efforts should also be made to prevent and control longitudinal cracks. The main conclusions of this study are as follows:

(1) The discrete characteristics and variance distribution characteristics of road surface deformation can be used to describe the degree of activity of the vertical deformation and to establish an activity index.
(2) The time series elevation variance and standard deviation of elevation change of road surface deformation were analyzed to construct an activity index, used to describe the activity of road points, sections, longitudinal lines, intervals, and longitudinal deformation.
(3) Vertical deformation activity was significantly correlated with longitudinal crack condition, distribution, and development characteristics. Longitudinal activity was used to describe the activity of vertical deformation in a longitudinal line of the road surface. The mean value of the activity of adjacent longitudinal lines was used to describe the activity of vertical deformation in a transverse interval. Longitudinal activity was used to describe the average condition of longitudinal activity in a section or several sections.
(4) The activity was greatest in each monitoring section from March to May. From Aug. to Jan., during the period of thermal expansion and frost heave, activity was relatively greater. The longitudinal activity varied significantly between sections, with numerical differences reaching 3 to 4 times.
(5) The relationship between activity and longitudinal crack condition was analyzed. There was a correlation between crack length and total activity in the interval. The greater the activity, the greater the longitudinal crack length, and the two followed an exponential relationship.
(6) An analysis of the activity and its relationship with the development of longitudinal cracks in different periods indicates that there was a logarithmic relationship between the annual growth length of longitudinal cracks and the relationship between the longitudinal activity of the section. The greater the activity, the greater the annual growth length of longitudinal cracks. The activity from Feb. to May shows a linear relationship with the development rate of longitudinal cracks.

Author Contributions: Conceptualization, H.W. and L.J.; methodology, H.Z.; validation, Y.L. and H.W.; formal analysis, L.J.; investigation, Y.L.; data curation, Y.T. and L.X.; writing—original draft preparation, H.W. and L.J.; funding acquisition, H.W. All authors have read and agreed to the published version of the manuscript.

Funding: This research received no external funding.

Institutional Review Board Statement: Ethical review and approval were waived for this study, due to the fact that no human subjects were involved.

Informed Consent Statement: Not applicable.

Data Availability Statement: The data that support the findings of this study are included within the article.

Acknowledgments: The authors would like to thank Zhao Zhenguo, Chief Engineer of Heilongjiang Provincial Institute of Transportation Planning, Survey, and Design Group Co., Ltd. for helpful discussions on topics related to this work.

Conflicts of Interest: The authors declare no conflict of interest.

References

1. Feng, D.-C.; Lin, B.; Zhang, F.; Feng, X. A review of freeze-thaw effect on soil geotechnical properties. *Sci. Sin. Technol.* **2017**, *47*, 111–127. [CrossRef]
2. Rivière, A.; Jost, A.; Gonçalvès, J.; Font, M. Pore water pressure evolution below a freezing front under saturated conditions: Large-scale laboratory experiment and numerical investigation. *Cold Reg. Sci. Technol.* **2019**, *158*, 76–94. [CrossRef]
3. Zhao, T.; Zhang, M.; Lu, J.; Yan, Z. Correlation between ground surface deformation and influential factors in permafrost regions. *J. Harbin Inst. Technol.* **2021**, *53*, 145–153.
4. Batenipour, H.; Alfaro, M.; Kurz, D.; Graham, J. Deformations and ground temperatures at a road embankment in northern Canada. *Can. Geotech. J.* **2015**, *51*, 260–271. [CrossRef]
5. Wang, J. *Study on Deformation Characteristics of Embankment of Overly Wet Soil in Reconstruction and Extension of Old Road in Seasonal Frozen Area*; Northeast Forestry University: Harbin, China, 2018.
6. Liang, B.; Wei, C.; Zhang, X.; Zhang, P. Prediction of Frost Heave Deformation of High-speed Railway Subgrade Based on Dynamic GM-Markov Optimization Model. *Subgrade Eng.* **2022**, *4*, 7–12.
7. Luo, X.; Yu, Q.; Ma, Q.; Guo, L. Study on the heat and deformation characteristics of an expressway embankment with shady and sunny slopes in warm and ice-rich permafrost regions. *Transp. Geotech.* **2020**, *24*, 100390. [CrossRef]
8. Hu, T.; Wang, L. Ground source heat pump heating of embankments in cold regionsto eliminate frost heave. *J. Tsinghua Univ. (Sci. Technol.)* **2022**, *62*, 871–880.
9. He, B. Experimental Study on Frost Heaving Characteristics of the Embankment Filler of Jungar Banner-Shenchi Railway. *J. Water Resour. Archit. Eng.* **2022**, *20*, 160–165+216.
10. Zhang, H.T.; Yang, L.Q.; Guo, F. Solution and Analysis of Dynamic Response for Layered Pavement Structure Based on PIM. *J. Chongqing Jiaotong Univ. (Nat. Sci.)* **2022**, *41*, 82–91.
11. Liang, N. *Study on the Deformation and Stability of Highway Embankment in Permafrost Region under the Condition of Climate Warming*; Chongqing Jiaotong University: Chongqing, China, 2018.
12. Wang, Y.; Peng, C. Prevention and control technology of longitudinal cracks at new and old road splices in highway widening projects. *Transp. World* **2019**, 65–66.
13. Zhang, C.; Wang, H.; You, Z.; Ma, B. Sensitivity analysis of longitudinal cracking on asphalt pavement using MEPDG in permafrost region. *J. Transp.-Tion Eng. Engl. Ed.* **2015**, *2*, 40–47. [CrossRef]
14. Cao, J.; Shen, T.; Li, R. Analysis of longitudinal cracks in asphalt pavement of highway reconstruction and expansion in severe cold interval. *Highway* **2021**, *66*, 368–371.
15. Zhou, J. Investigation, Investigation Analysis and Research of Typical Diseases of Longitudinal Cracks on Expressways in Liaoning Province. *North. Commun.* **2019**, *12*, 51–54.
16. Chang, Y.; Yu, Q.; You, Y.; Guo, L. Formation mechanism of longitudinal cracks in expressway em-bankments with inclined thermosyphons in warm and ice-rich permafrost regions. *Appl. Therm. Eng. Des. Process. Equip. Econ.* **2017**, *133*, 21–32. [CrossRef]
17. Chai, M.; Mu, Y.; Zhang, J.; Ma, W.; Liu, G.; Chen, J. Characteristics of Asphalt Pavement Damage in De-grading Permafrost Regions: Case Study of the Qinghai–Tibet Highway, China. *J. Cold Reg. Eng.* **2018**, *32*, 05018003. [CrossRef]
18. Linares C, M. Effect of freeze-thaw cycles on low temperature performance of asphalt mixtures. *Transp. Res. Procedia* **2020**, *48*, 3634–3641.
19. Li, G.Y.; Ma, W.; Wang, F.; Mu, Y. Processes and mechanisms of multi-collapse of loess roads in seasonally frozen ground regions: A review. *Sci. Cold Arid. Reg.* **2015**, *7*, 456–468.
20. Liu, J.; Tai, B.; Fang, J. Ground temperature and deformation analysis for an expressway embankment in warm permafrost regions of the Tibet plateau. *Permafr. Periglac. Process.* **2019**, *30*, 208–221. [CrossRef]
21. Simonsen, E.; Isacsson, U. Thaw weakening of pavement structures in cold regions. *Cold Reg. Sci. Technol.* **1999**, *29*, 135–151. [CrossRef]
22. Cheng, Y. *Deformation Monitoring Technology and Stability Evaluation of Silty Clay Subgrade in Seasonal Frozen Region*; Northeast Forestry University: Harbin, China, 2021.

23. Zhang, Y.; Yang, W.; Li, R.; Zhao, W.; Zhang, G.; Li, P. Monitoring and Rule Analysis of Frost Heaving and Thawing Settlements of Heavy Haul Railway Roadbedin Seasonal Frozen Region. *China Railw. Sci.* **2022**, *43*, 1–10.
24. Long, X.; Shen, G.; Cai, L.; Liu, J. Hydro-thermal coupling model test and field validation of uneven frost heave of pavement structure. *J. Harbin Inst. Technol.* **2019**, *51*, 172–178.